

高熱流束プール沸騰における加熱面温度分布と発泡点密度の数値解析

Numerical Study of Spatial Surface Temperature and Nucleation Site Density At High Heat Flux Pool Boiling

賀纒 (東大工院) 伝正 庄司 正弘 (東大工) 伝正 丸山 茂夫 (東大工)

Ying He, Masahiro Shoji and Shigeo Maruyama

Dept. of Mech. Eng., The Univ. of Tokyo, Hongo 7-3-1, Bunkyo-ku, Tokyo, 113-8656

A numerical study of nucleation site density was included into the macrolayer model of Maruyama et al.^[5]. The results indicate that nucleate boiling curve and critical heat flux point move to the lower superheat region with increasing surface roughness, which is in a good agreement with Bereson^[1]'s experiment. Furthermore, a three dimensional numerical method using finite control volume method and implicit numerical method was developed to explore spatial and temporal variations on surface temperature. The results show that the temperatures at the interface of vapor stem and liquid layer change sharply, whereas the temperatures at the areas that are only occupied by vapor stem and liquid vary smoothly.

Key Words: Numerical Study, Pool Boiling, Surface Temperature, Nucleation Site Density

INTRODUCTION

The macrolayer is widely used in numbers of models for nucleate pool boiling and CHF. Maruyama et al. ^[5] put forward a numerical macrolayer model. Later, the present authors developed this model with different numerical methods ^{[2][3]}. Although the models successfully predicted boiling curve at steady state and transient heating, the effect of nucleation site density was not considered in the models. Some theoretical and experimental work has shown that active site density may play a role in high heat flux nucleate boiling and CHF. Thus, it is necessary to consider the discrete bubble behavior in the numerical model.

On the other hand, spatial and temporal variations of surface temperature are found to be significant. Kenning^[4] pointed out that spatial and temporal variations in surface temperature could occur considerably. Pasamehmetoglu^[6] reported there was a sharp temperature increases while a single bubble is growing. Subsequently, several investigators simulated surface temperature variations at low heat flux nucleate boiling regime and a single bubble. Sadasivan et al. ^[7] presented nonlinear effects in high heat flux nucleate boiling. They modeled the problem domain comprised of the macrolayer and heater and associated with the individual behavior of nucleation sites on the heater surface. They revealed that surface-averaged temperatures had nonlinear period-doubling behavior.

In the present study, the effect of surface roughness and the spatial instantaneous temperature distributions were explored. By including the simulation of individual behavior of nucleation site, we obtained different boiling curves under different surface conditions. Moreover, associating the three-dimensional modeling of temperature field in the wall with the developed macrolayer, we explored the spatial and temporal variations of surface temperature. We will first describe the simulation of the nucleation site.

SIMULATION OF NUCLEATION SITE

So far, there're few studies to characterize the site density quantitatively. Wang & Dhir^[9] put forward a correlation about cavity densities and cavity diameters as the followings:

$$N_s (\text{sites} / \text{cm}^2) = \begin{cases} 9.0 \times 10^3 D_c^{*-2.0} & D_c^* \geq 5.8 \text{mm} \\ 10.3 + 2.4 \times 10^6 D_c^{*-5.2} & 3.5 \leq D_c^* < 5.8 \text{mm} \\ 2213.5 + 1.0 \times 10^6 D_c^{*-5.4} & D_c^* \leq 3.5 \text{mm} \end{cases} \quad (1)$$

According to the above correlation, the cavity density will be so large that it is difficult to be simulated by the present computer. Hence, we employed the following method:

1. The number of surface cavities is set to vary from 150 to 600.

2. By referring to Equation (1), we set that the cavity diameters were less than 7.0 μm . Among them, 1~5% of the surface cavities was between 5.8~7.0 μm , 9~20% was between 3.5~5.8 μm and 75~90% was less than 3.5 μm .

3. The site spatial distribution and diameter are assigned randomly by satisfying the conditions in step (2).

The simulated cavities were assigned and distributed in the 21 \times 21 subdivisions. In some meshes, there were several cavities, in some others, there was only one cavity, and in the left meshes, there were no cavities. For the simplification, we assumed that there was at most one cavity in on mesh and only the biggest one was chosen to be the potential nucleation site. Consequently, a part of assigned cavities are selected to be the potential nucleation sites. Hence, the corresponded active wall superheat could be obtained from the following expression,

$$\Delta T_{act} = \frac{2sT_{sat}}{r_v H_{fg} R_{ca}} \quad (2)$$

Where R_{ca} is the cavity mouth radius.

When a certain power was input to the heater, some part of potential nucleate sites became activated and formed vapor stems instantaneously. Later, combining the macrolayer model described before ^{[2][3]}, we could find the wall superheat corresponded to the input heat flux.

Figure 1 shows the predicted boiling curves for different surface conditions. As displayed that, with the number of cavities increasing, the boiling curves moved the lower superheat region, whereas the CHF value didn't change so much. When the number of surface cavities was 600, for relatively rougher surface, the boiling curve shifted to the left of that with smother surface.

SPATIAL AND TEMPORAL SURFACE TEMPERATURE

Governing Equations

The three-dimensional transient heat conduction was considered in this part of study. Boiling process was included through boundary conditions. The transient heat conduction is described in Cartesian coordinates as

$$\frac{\partial T}{\partial t} = a \left(\frac{\partial^2 T}{\partial x^2} + \frac{\partial^2 T}{\partial y^2} + \frac{\partial^2 T}{\partial z^2} \right) + \frac{w}{rc} \quad (3)$$

Subject to the following boundary and initial conditions:

$$x=0 \quad \text{and} \quad x=L \quad \text{for all } y, z, t \quad \frac{\partial T}{\partial x} = 0 \quad (4)$$

$$y=0 \quad \text{and} \quad y=L \quad \text{for all } x, z, t \quad \frac{\partial T}{\partial y} = 0 \quad (5)$$

$$z=H, \text{ either } T=T_b \text{ or } -I_H \frac{\partial T}{\partial z} = q_{in} \quad (6)$$

$$z=0, \quad q_s(i, j) = -I_H \left(\frac{\partial T}{\partial z} \right) \quad (7)$$

The first four boundary conditions for the y and x directions are referred to as a rectangular heater with an insulated periphery, or a representative rectangular portion of the total heater where the periphery acts as a symmetry line. The boundary conditions of the bottom surface of the heater are shown in Equation (7). In this equation, (a) a constant temperature (T_b) or (b) a constant heat flux (q_{in}) is prescribed at the bottom surface as the boundary condition. For these two conditions, the heat generation term w/r_c in equation (4) is set to zero. Equation (8) shows the boundary condition the top of heater. Because the top of the heater is the boiling surface, the boiling effects are included through calculating the local surface heat flux of boiling. The local surface heat flux $q_s(i, j)$ can be calculated by the macrolayer model^[2]. Specifically, $q_s(i, j)$ can be expressed as the following

$$\begin{aligned} q_s(i, j) &= r_l H_{fg} \left(-\frac{dw(i, j)}{dt} \right) \\ &= r_l H_{fg} (1 - a_b(i, j)) \left(-\frac{d\mathbf{c}(i, j)}{dt} \right) + r_l H_{fg} \mathbf{c}(i, j) \frac{da_b(i, j)}{dt} \\ &= q_{ab}(i, j) + q_{cd}(i, j) \end{aligned} \quad (8)$$

In addition, the initial condition is specified as

$$T_s^0(i, j) = T_0 \quad (9)$$

T_0 is wall temperature corresponded to the input heat flux, which can be gained from the simulated boiling curve. The initial temperature profile inside the heater is calculated by one-dimensional steady state heat conduction, i.e.

$$T^0(i, j, k) = T_s^0(i, j) + \frac{I \Delta z}{I_H} q_{in} \quad (10)$$

The fully implicit scheme was employed to the three-dimensional heat transfer problem. The calculation is stable when the following condition is satisfied:

$$t \Delta T_t \leq (t + \Delta t) \Delta T_{t+\Delta t} \quad (11)$$

Main Results

Figure 2a shows the surface patterns at 0.5 and 30ms when the heat flux was 1.57 MW/m^2 and the thickness of the heater was 1mm. Figure 2b gives the temperature variations of five points plotted in Figure 3a within two bubble departure periods. We can see that, when vapor and liquid filled with the grids at the same time, the temperatures in these points were generally lower; when only vapor or liquid occupied the grids, the temperature were relatively higher.

Figure 3 provides the local instantaneous temperatures on the whole surface at 0.5 and 30ms. As revealed that, the surface temperatures remained almost the same at the initial stage of the hovering period, with the time increasing, the area that liquid and vapor intersected became more, thus, the local surface temperature became significantly large.

SUMMARY AND CONCLUSIONS

1. By considering nucleation from the cavities on a heated surface, boiling curves at different surface conditions were obtained. The results well reproduced the roughness effects reported by Bereson.
2. The three-dimensional transient heat transfer process was considered to examine the spatial and temporal variations on surface temperature. The simulated results indicate that the local surface temperature fluctuations are considerably large and the temperatures at the interface of vapor stem and liquid change steeply.

REFERENCE

(1) Berenson, P. J., M.I.T Heat Transfer Lab. Tech. Rep.17 (1960). (2) He, Y., et al., Convective Flow and Pool Boiling Conference, Session : Mathematical Simulation of Boiling, Kloster Irsee (1997). (3) He, Y., et al., 35th National Heat Transfer Symposium of Japan, pp.913-914 (1998). (4) Kenning, D. B. R., Proc. of Eng. Foundation Conf., pp.79-82 (1992). (5) Maruyama, S., et al., Proc. of the 2nd JSME-KSME Thermal Eng. Conf., pp.3-345-3-348(1992). (6) Pasamehmetoglu, K. O., Numerical Heat

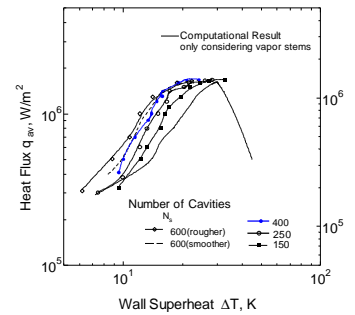


Figure 1 Predicted Boiling Curves for Different Surface Conditions

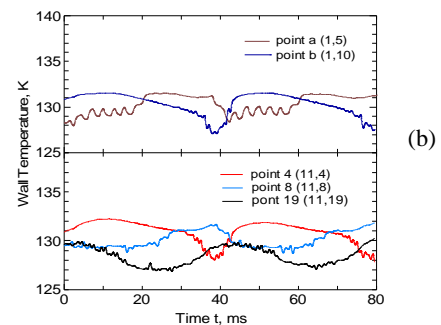
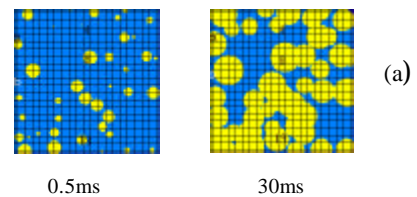


Figure 2(a) Instantaneous Surface Dry Pattern
(b) Temporal Variations of Instantaneous Wall Temperatures For Different Positions ($q=1.57 \text{ MW/m}^2$, $H=1 \text{ mm}$)

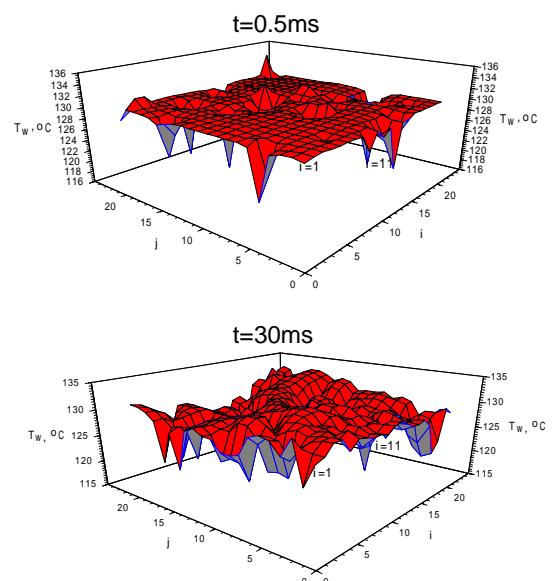


Figure 3 Local Instantaneous Temperatures on the Heated Surface ($q=1.57 \text{ MW/m}^2$, $H=1 \text{ mm}$)

Sadasivan, P., et al., Trans. ASME, J. Heat Transfer, Vol. 117, pp.981-989 (1995). (8) Shoji, M., Third Int. Conf. on Multiphase Flow, 0.2-14, Lyon, France (1998). (9) Wang, C. H. and Dhir, V. K., Trans. ASME, J. Heat transfer, Vol. 115, pp.659-669 (1993).